Journal of Applied Electrochemistry **30**: 1415–1420, 2000.

Study of cerium species in molten Li_2CO_3–Na_2CO_3 in the conditions used in molten carbonate fuel cells. Part II: Potentiometric and voltammetric behaviour[†]

M. CASSIR*, V. CHAUVAUT, A. ALFARRA and V. ALBIN
Ecole Nationale Supérieure de Chimie de Paris, Laboratoire d'Electrochimie et de Chimie Analytique (UMR 7575 du CNRS), 11 rue Pierre et Marie Curie, 75231 Paris Cedex 05, France
*(*author for correspondence, fax: (+33) 1 44 27 67 50, e-mail: cassir@ext.jussieu.fr)*

Received 31 July 1999; accepted in revised form 11 January 2000

Key words: cerium, cerium oxide, fuel cell, molten carbonate, potentiometry, voltammetry

Abstract

The electrochemical behaviour of metallic cerium and cerium dioxide is analysed in molten Li_2CO_3–Na_2CO_3 under the anodic and cathodic conditions used for the molten carbonate fuel cells (MCFC). Chronopotentiometric measurements on metallic cerium rods or foils show the influence of CeO_2 growth and the deviation from its stoichiometric composition. A study of the voltammetric characteristics of dissolved cerium at a gold electrode, of metallic cerium and cerium oxide is carried out in both oxidising and reducing MCFC atmospheres. Experimental evidence is given for the existence of a solid–solid cerium system: $Ce_2O_3(s)|CeO_2(s)$ and a system relative to dissolved cerium species $Ce_2O_3(l)|CeO_2(l)$. These systems are in agreement with thermodynamic predictions. Other more complex phenomena involving interactions with alkali species are discussed.

1. Introduction

The interest in cerium oxide as an alternative material for MCFC bipolar coating, anode or inert support for the electrolyte has been outlined in a previous paper [1]. In Part I of this series, different aspects were investigated [1]. CeO_2 is the thermodynamically stable cerium species in molten Li_2CO_3–Na_2CO_3 under anode and cathode standard conditions, but a partially solubility of Ce_2O_3 can be predicted. The solubility of cerium in the mentioned eutectic is about 3×10^{-4} to 5×10^{-4} mol kg^{-1} depending on the experimental conditions. Surface analysis of CeO_2 pellets by X-ray diffraction and X-ray photoelectron spectroscopy confirmed the stability of CeO_2, showed the presence of Ce(III) and the possible incorporation of sodium species in the CeO_2 lattice.

As far as we know no electrochemical data can be found in the literature on cerium redox systems in molten carbonates. The aim of this work is to study the electrochemical behaviour of cerium in the mentioned carbonate eutectic and more specifically under anode conditions. The open-circuit potential of a cerium or cerium oxide electrode is followed under the usual anode equilibrium conditions (H_2 + CO_2, 80:20, humidified with water heated at 60 °C). The voltammetric behaviour of cerium is characterised by comparing the results at different electrodes: gold, metallic cerium and CeO_2 under anode and cathode (air + CO_2, 70:30) standard atmospheres.

2. Experimental details

Reagents, anodic and cathodic gas atmospheres and the electrochemical cell were fully described in Part 1 [1] and in previous papers [2, 3]. The reference electrode was a silver wire dipped into an Ag_2SO_4 (10^{-1} mol kg^{-1}) Li_2CO_3–Na_2CO_3 eutectic and the auxiliary electrode was a gold wire. The working electrodes were either a gold wire of diameter 1 mm, metallic cerium rods of 7×40 mm^2, cerium foils of $10 \times 10 \times 0.25$ mm^3 (Goodfellow, 99.9% of purity), or cerium oxide pellets of 12×4 mm^2, with 99.9% purity grade, provided by Cerac.

All the cerium or cerium oxide working electrodes were connected to a gold wire (1 mm dia.). Each working electrode was introduced in the cell and exposed to the gaseous atmosphere above the molten salt for 36 h, a time necessary for reaching the gas equilibrium, before immersion in the melt. CeO_2 powder (particles <5 μm), of analytical purity, 99.9%, was provided by Aldrich. Electrochemical measurements were carried out with an EGG potentiostat system, model 263 A, controlled by a computer.

[†] Dedicated to the memory of Daniel Simonsson

3. Results and discussion

3.1. *Potentiometric measurements*

The open-circuit potential of a gold electrode dipped in the Li_2CO_3–Na_2CO_3 melt with no cerium present, under the standard anode conditions, rapidly reached a stable potential of −1 V ($Ag|Ag^+$) attributable to the $H_2|H_2O$ and $CO|CO_2$ systems occurring at very close potentials [7]. The situation was very different in the case of metallic cerium (rod or foil) or cerium oxide working electrodes immersed in molten Li_2CO_3–Na_2CO_3, at 650 °C under a standard anode atmosphere, as can be seen in Figure 1. The results obtained for the metallic cerium electrodes were similar. Cerium in contact with air is spontaneously oxidized and recovered by an oxide layer before immersion in the carbonate melt. Visually, the cerium foil was more shiny, which means that the thickness of the oxide layer was smaller than in the case of the cerium rod. The initial open-circuit potential was −0.4 V ($Ag|Ag^+$) for the cerium rod and 0 V ($Ag|Ag^+$) for foil. In both cases the first tendency is a decrease in potential which is attributable to change in the stoichiometric composition of CeO_2 at 650 °C: an oxygen deficient oxide, CeO_{2-x}, can be formed at such high temperatures [4, 5]. The potential was stable for about 800 min for the rod and 100 min for the foil, probably indicating the existence of two simultaneous phenomena: oxidation of the metal, combined with decomposition of CeO_2 into the nonstoichiometric oxide. Afterwards, the potential dramatically increased in the first case (Figure 1(a)) and slightly in the second one (Figure 1(b)). This increase may be due to the oxidation of Ce to CeO_2. After 36 h, the potential had not stabilised which means that, in spite of the oxide layer already formed, the oxidation process was still going on. It can be deduced that the oxide layer was relatively porous and did not protect the metal from further oxidation. In the case of CeO_2 pellet, as presented in Figure 1(c), the open-circuit potential was registered for 36 h. This potential decreased for one hour and reached a relatively stable potential at about −0.1 V ($Ag|Ag^+$). This decrease may correspond to the progressive decomposition at 650 °C of CeO_2 to nonstoichiometric CeO_{2-x}, with $10^{-4} < x < 10^{-3}$ [5], or be caused by the chemical insertion of alkali cations [1] or from both phenomena.

In effect, from a crystallographic viewpoint, CeO_2 has a face-centred cubic structure, with a lattice parameter $a = 5.4113$ Å and a density of 7.3. This structure has possible octahedral insertion sites in the middle of each edge and in the cube centre. The O^{2-} radius with a coordination number of 4 is about 1.24 Å and that of Ce^{4+} with a coordination number of 8 is about 1.11 Å [6]. Thus, the CeO_2 lattice is not so compact and may allow the insertion of alkali cations.

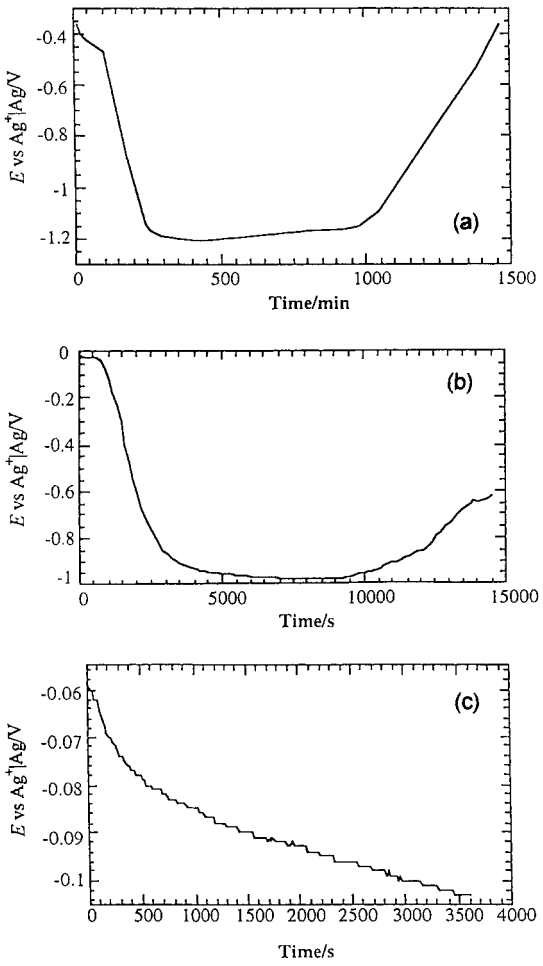

Fig. 1. Open-circuit potential of different electrodes in Li_2CO_3–Na_2CO_3 at 650 °C under $H_2 + CO_2$, 80:20, humidified with water heated at 60 °C. (a) cerium rod of 7×40 mm^2; (b) cerium foil of $10 \times 10 \times 0.25$ mm^3; (c) CeO_2 pellet of 12×4 mm^2.

3.2. *Voltammetric study at a gold electrode*

3.2.1. *Anodic conditions*

The electrochemical stability domain of Li_2CO_3–Na_2CO_3 at 650 °C in standard anode MCFC conditions is shown in Figure 2. Its extent is about 1.9 V, from the reduction of Na^+ at −1.7 V ($Ag|Ag^+$) to the oxidation

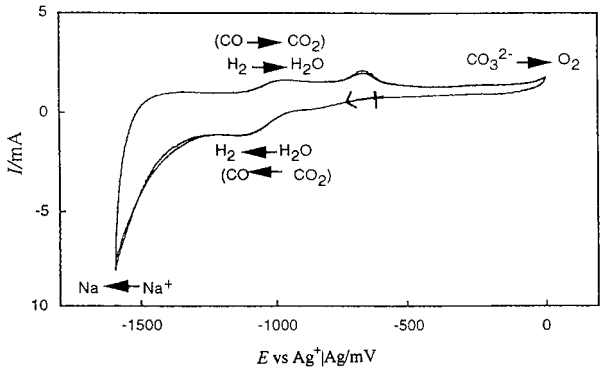

Fig. 2. Cyclic voltammogram representing the electrochemical stability domain of molten $Li_2CO_3 + Na_2CO_3$ at a gold electrode (wire of 1 mm dia.), at 650 °C, under $H_2 + CO_2$, 80:20, humidified with water heated at 60 °C. $v = 100$ mV s^{-1}; start potential, −0.6 V ($Ag|Ag^+$).

of CO_3^{2-} at 0.2 V ($Ag|Ag^+$). The system appearing at −0.98 V ($Ag|Ag^+$) and −1.1 V ($Ag|Ag^+$) is characteristic of H_2/H_2O, but can also result from a competition with the CO/CO_2 system, as described elsewhere [7]. The anodic peak at about −0.7 V ($Ag|Ag^+$) is most probably due, according to the interpretation of Mugikura and Selman [8], to the reaction of H_2 with the sulfur contained in the Viton O-rings to form H_2S which dissolves to S_2, exhibiting the extra oxidation peak.

Experiments were carried out in Li_2CO_3–Na_2CO_3 eutectic at 650 °C containing CeO_2 powder (10^{-1} mol kg^{-1}) and CeO_2 pellets. The voltammogram obtained after 24 h in a melt containing CeO_2 powder and shown in Figure 3, exhibits, apart from the systems identified in the study of the electrochemical stability domain, an electrochemical system a–a′ appearing at an oxidation potential of −1.35 V ($Ag|Ag^+$) and a reduction potential of −1.4 V ($Ag|Ag^+$), with an appearance characteristic of solid species present at the electrode. Moreover, close to these peaks, another system appears, which is not observed in the absence of CeO_2 in the melt. This b–b′ system has a reduction peak at −1.23 V ($Ag|Ag^+$) and an oxidation peak at −1.19 V ($Ag|Ag^+$). The shape of these peaks is characteristic of soluble species. Another reduction peak, c, can also be seen at −1.54 V ($Ag|Ag^+$), which again only appears after the addition of CeO_2. A study of the influence of scan rate on the mentioned systems was attempted, but the peak intensities dramatically decreased after three or four successive scans. In the case of the a–a′ system, it seems that the solid present at the electrode becomes less adherent after imposing successive negative and positive overpotentials. Similar results were obtained when adding a CeO_2 pellet to the melt. However, as can be seen in Figure 4, peak intensities are lower than in the case of powder addition and the system b–b′ is less defined. The development of the a–a′ system with scan rate showed that the respective potentials are independent of scan rate. This indicates that, in the case of the pellet, solid species are more adherent to the electrode. In both experiments two phenomena occurred: part of the cerium oxide dissolved and deposited at the electrode surface. In the case of the powder, crystals of CeO_2 may be directly deposited at the electrode surface which increases the current intensity. But this deposit is certainly less adherent than in the case of pellet dissolution because of the larger particle size.

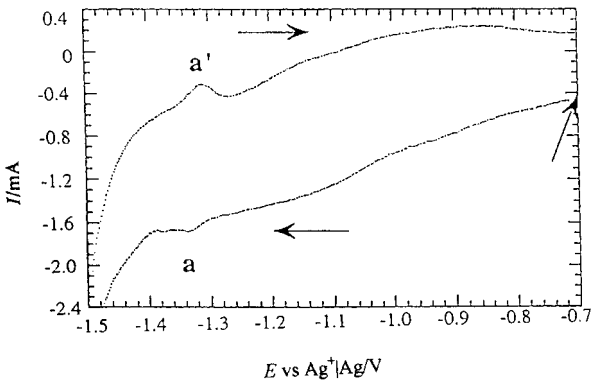

Fig. 4. Cyclic voltammogram at a gold electrode of molten Li_2CO_3 + Na_2CO_3 containing CeO_2 pellet (12 × 4 mm^2), at 650 °C, under H_2 + CO_2, 80:20, humidified with water heated at 60 °C. v = 100 mV s^{-1}; start potential, −0.70 V ($Ag|Ag^+$).

3.2.2. *Cathodic conditions*

The same voltammetric study was carried out under standard cathode conditions. In the case of the CeO_2 pellet addition, as shown in Figure 5, the system b–b′ was observed at −1.2 V ($Ag|Ag^+$) for the reduction peak and at −1.15 V ($Ag|Ag^+$) for the oxidation peak. The other peaks are difficult to identify. The dependence of the peak currents on scan rate was not conclusive because of their low intensity and poor definition. The voltammogram obtained after adding the CeO_2 powder is presented in Figure 6. Most of the former peaks are not visible, because they are probably occurring after the reduction limit. In contrast to the situation for anodic environment, the oxidation peak b′ is relatively well defined. This may be due to the change in the morphology and stability of the deposited CeO_2 on gold. Current b′ is proportional to v, as shown in

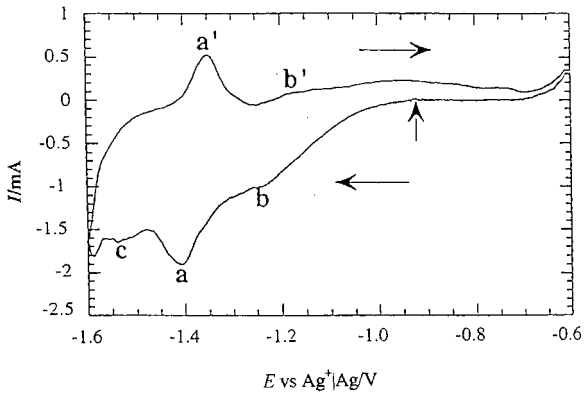

Fig. 3. Cyclic voltammogram at a gold electrode of molten Li_2CO_3 + Na_2CO_3 containing CeO_2 powder (10^{-1} mol kg^{-1}), at 650 °C, under H_2 + CO_2, 80:20, humidified with water heated at 60 °C. v = 20 mV s^{-1}; start potential, −0.92 V ($Ag|Ag^+$).

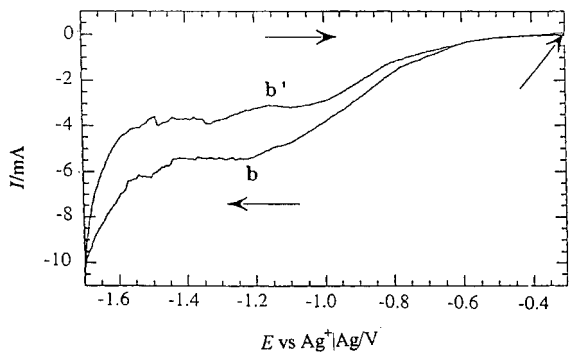

Fig. 5. Cyclic voltammogram at a gold electrode of molten Li_2CO_3 + Na_2CO_3 containing CeO_2 pellet (12 × 4 mm^2), at 650 °C, under air + CO_2, 70:30. v = 100 mV s^{-1}; start potential, −0.30 V ($Ag|Ag^+$).

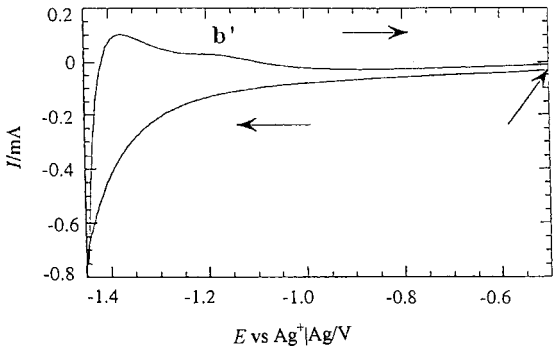

Fig. 6. Cyclic voltammogram at a gold electrode of molten Li_2CO_3 + Na_2CO_3 containing CeO_2 powder (10^{-1} mol kg^{-1}), at 650 °C, under air + CO_2, 70:30. v = 100 mV s^{-1}; start potential, −0.50 V ($Ag|Ag^+$).

Figure 7, but the peak potentials become more positive with increasing scan rate. It can be concluded that b–b′ system is not rapid and most probably corresponds to a dissolved cerium species.

3.2.3. *Interpretation*

Potential–acidity diagrams, established on the stability of cerium in Li_2CO_3–Na_2CO_3 in a previous paper [1], showed that CeO_2 is stable over the whole electrochemical stability domain under both anodic and cathodic conditions. The only redox system observed in the theoretical electrochemical window is $Ce_2O_3|CeO_2$. According to this thermodynamic prediction, the solid–solid a–a′ system can be attributed to the following reaction:

$$2\,CeO_2(s) + CO_2 + 2\,e^- \rightarrow Ce_2O_3(s) + CO_3^{2-} \qquad (1)$$

Scanning electron microscopy analysis (SEM) coupled with energy distribution spectroscopy (EDS) showed the presence of small crystals compounds of cerium and oxygen at the surface of the gold electrode. In the case of the b–b′ system, this may result from the redox reaction of the dissolved cerium species. In effect, a first dissociation step of CeO_2 could be followed by the reduction of Ce^{4+}:

$$CeO_2 + 2\,CO_2 \rightarrow Ce(CO_3)_2 \rightarrow Ce^{4+} + 2\,CO_3^{2-} \qquad (2)$$

$$Ce^{4+} + e^- \rightarrow Ce^{3+} \qquad (3)$$

At this stage, it is difficult to explain the origin of c peak. It may result from the electrochemical insertion of an alkali species in the CeO_2 lattice yielding an unstable species, because no reoxidation current was observed.

3.3. *Voltammetric study at a CeO_2 electrode*

The voltammogram obtained at a CeO_2 electrode immersed in Li + Na carbonate eutectic is shown in Figure 8. It was necessary to use higher scan rate of 10 V s^{-1} to observe all the possible redox phenomena. Three oxidation peaks were observed:

(i) *Peak C*, at −1.6 V ($Ag|Ag^+$), represents the reoxidation of sodium formed by the reduction of Na^+.

(ii) *Peak A′*, at −1.2 V ($Ag|Ag^+$), seems to correspond to the a′ peak, or Ce_2O_3 oxidation, observed at a gold electrode; the reduction of CeO_2 occurring close to the reduction limit cannot be observed. The development of this peak with scan rate showed no precise tendency, probably because of the low conductivity of the CeO_2 electrode. In order to determine the reduction potential of CeO_2, scan rates of 10 V s^{-1}, with 5 s stop at different reversal potentials, were investigated. Figure 9 shows that this reduction potential is localised at −1.45 V ($Ag|Ag^+$).

(iii) *Peak D*, at −0.4 V ($Ag|Ag^+$), only appeared when the reversal potential was lower than −1.5 V ($Ag|Ag^+$). A hypothesis concerning this peak will be presented later.

3.4. *Voltammetric study at metallic cerium electrodes*

Cyclic voltammograms were obtained at a cerium rod or a cerium foil in anodic conditions, as shown in Figures 10 and 11, respectively. The peak currents obtained at the cerium rod are significantly higher than for the cerium foil. In effect, the contact surface is significantly

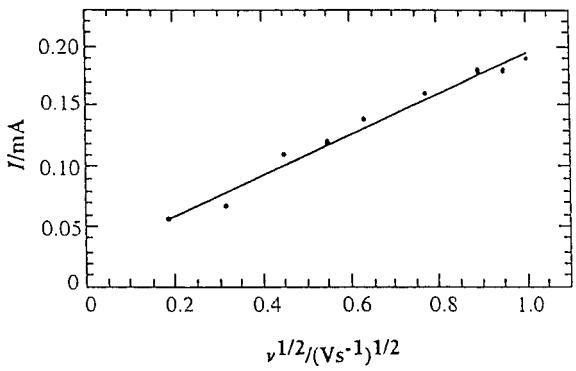

Fig. 7. Development of peak current b′ with v in the conditions given in Figure 7.

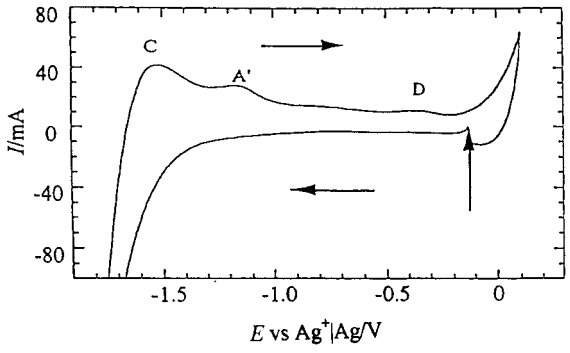

Fig. 8. Cyclic voltammogram at a CeO_2 electrode (12 × 4 mm^2) in Li_2CO_3–Na_2CO_3, at 650 °C, under H_2 + CO_2, 80:20, humidified with water heated at 60 °C. v = 5 V s^{-1}; start potential, −0.12 V ($Ag|Ag^+$).

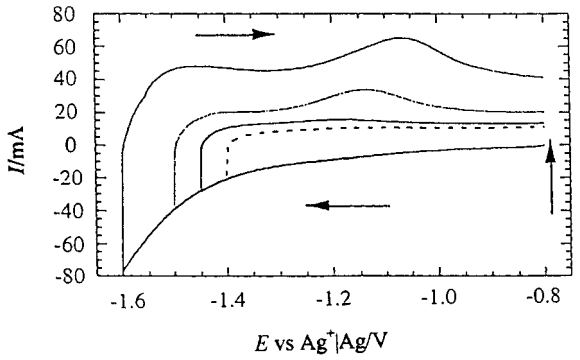

Fig. 9. Cyclic voltammograms at a CeO_2 electrode (12×4 mm^2) in Li_2CO_3–Na_2CO_3, at 650 °C, under $H_2 + CO_2$, 80:20, humidified with water heated at 60 °C. $v = 10$ V s^{-1}; start potential, −0.78 V ($Ag|Ag^+$). Stop of 5 s at different reversal potentials: −1.60; −1.50; −1.45; −1.40 V ($Ag|Ag^+$).

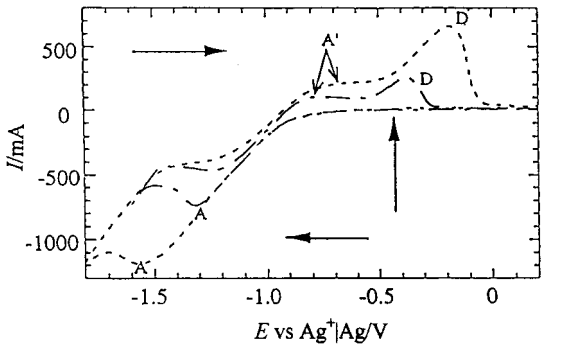

Fig. 10. Cyclic voltammograms at a cerium rod (7×40 mm^2) in Li_2CO_3–Na_2CO_3, at 650 °C, under $H_2 + CO_2$, 80:20, humidified with water heated at 60 °C. Scan rates, $v = 20$ and 80 mV s^{-1}; start potential, −0.43 V ($Ag|Ag^+$).

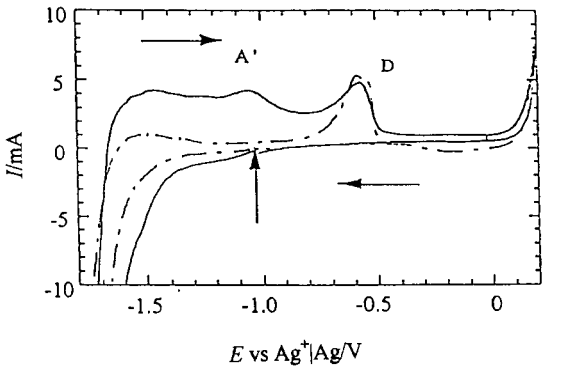

Fig. 11. Cyclic voltammograms at a cerium foil ($10 \times 10 \times 0.25$ mm^3) in Li_2CO_3–Na_2CO_3, at 650 °C, under $H_2 + CO_2$, 80:20, humidified with water heated at 60 °C. Scan rates, $v = 10$ and 50 mV s^{-1}; start potential, −1.03 V ($Ag|Ag^+$).

larger with the cerium rod. At this electrode, the reduction peak A can be observed at a potential of −1.32 V ($Ag|Ag^+$) at low scan rate; its development with scan rate is linear, showing the behaviour of a solid species. This peak was not detected on the cerium foil or the cerium oxide electrodes. On both metallic cerium electrodes, peak A′ was observed. The A–A′ system corresponds in fact to the a–a′ system at the gold electrode. Peak A′ appears at an oxidation potential close to −1 V ($Ag|Ag^+$), a value more positive than in the case of the CeO_2 electrode (this shift could be due to the higher resistivity of CeO_2). According to thermochemical calculations and considering all the activities equal to 1, the equilibrium potential of the $Ce_2O_3|CeO_2$ system is −1.02 V ($Li_2O|O_2$) [1]. Knowing that Ce_2O_3 is not thermodynamically stable in molten carbonate and considering an activity of 10^{-3} for this species, the equilibrium potential becomes −0.74 V ($Li_2O|O_2$). Now, the interval between the theoretical reference $Li_2O|O_2$, used in thermodynamic calculations [1], and the experimental $Ag|Ag^+$ reference is about −0.7 V. Thus, a theoretical potential of −1.44 V ($Ag|Ag^+$) can be predicted. It corresponds approximately to the reduction potential of A peak.

Peak D is more intense in the case of metallic electrodes than for CeO_2. This peak may correspond to the oxidation of an M_xCeO_2 compound (with $M^+ = Na^+$ or Li^+). In effect, by the one hand, XPS measurements showed the possibility of a chemical insertion of sodium in the CeO_2 lattice [1]; the possible reaction being

$$CeO_2 + \frac{x}{2}Na_2CO_3 \Leftrightarrow Na_xCeO_2 + \frac{x}{2}CO_2 + \frac{x}{4}O_2 \quad (4)$$

On the other hand, the existence of a $LiCeO_2$ compound, with a monoclinic structure, has been reported in X-ray diffraction spectroscopic data [9]. It seems possible that $LiCeO_2$ and/or $NaCeO_2$ compounds are formed locally in CeO_2 dipped in molten carbonates. The existence of Ce(III) formed partially at the surface of the electrode is in agreement with this hypothesis [1]. The reaction may be the following:

$$CeO_2 + \frac{x}{2}M_2CO_3 \Leftrightarrow xMCeO_2 + (1-x)CeO_2 + \frac{x}{2}CO_2 + \frac{x}{4}O_2 \quad (5)$$

Experimentally, peak D is related to the phenomenon occurring at the reversal potential corresponding to the reduction limit which produces Na^+ ions. Therefore, the formation of a defined $NaCeO_2$ compound is likely, but no definitive proof exists at this stage.

Another possibility is the electrochemical intercalation of Li^+ or Na^+ in CeO_2, occurring at a potential slightly more negative than the reduction potential of CeO_2 to Ce_2O_3. In this case, peak D may be due to the deintercalation of alkali cations:

$$M_xCeO_2 \rightarrow CeO_2 + xM^+ + xe^- \quad (6)$$

This kind of intercalation–deintercalation phenomenon has already been described in the case of Li_2TiO_3 in molten carbonate [10] or Li_2TiO_7 [11]. An

electrochemical intercalation of Li^+ in CeO_2 has also been mentioned in nonaqueous media [12].

4. Conclusion

Potentiometric measurements can be correlated to the surface variation of metallic cerium or cerium oxide electrodes exposed to molten Li_2CO_3–Na_2CO_3 at 650 °C. The open-circuit potential is dependent on the decomposition of CeO_2 to a nonstoichiometric CeO_{2-x} compound in the case of the cerium oxide electrode. This phenomenon is combined with a progressive oxidation of the metal in the case of the metallic electrodes, cerium rod or cerium foil. The possibility of a chemical insertion of alkali cations may also have an influence on the open-circuit variation.

A comparative voltammetric study of cerium at a gold electrode and at metallic cerium electrodes in the same eutectic, under standard anodic and cathodic MCFC conditions, showed the presence of two systems in the electrochemical stability domain: a solid–solid redox reaction involving CeO_2(s) and Ce_2O_3(s) (confirmed by the presence of cerium oxide at the surface of the gold working electrode) and a system related to soluble species, $Ce^{3+}|Ce^{4+}$, proceeding from a previous dissolution of Ce^{4+} in the Li + Na carbonate eutectic. These results agree with previously established thermodynamic predictions. Another peak was attributed to the reoxidation of an alkali-cerium species produced close to the reduction limit. This peak could be due either to the oxidation of a defined $MCeO_2$ compound (with probably $M^+ = Na^+$) or to the deintercalation of alkali cations from the lattice of M_xCeO_2 compounds.

Acknowledgements

The authors thank Gaz de France (GDF/CNRS/ENSCP 414) and the European Community (Joule N°JOE3CT950024) for support. We also thank Dr J. Devynck, Dr B. Malinowska and H. Schneider.

References

1. V. Chauvaut, H. Schneider, V. Albin and M. Cassir, *J. Appl. Electrochem.* (2000) in press.
2. B. Malinowska, M. Cassir, F. Delcorso and J. Devynck, *J. Electroanal. Chem.* **389** (1995) 21.
3. M. Cassir, M. Olivry, V. Albin, B. Malinowska and J. Devynck, *J. Electroanal. Chem.* **452** (1998) 127.
4. J.R. Sims and R.N. Blumenthal, *High Temp. Sci.* **8** (1976) 99.
5. H.L. Tuller and A.S. Nowick, *J. Electrochem. Soc.* **126** (1979) 209.
6. R.D. Shannon, *Acta Cryst.* **A32** (1976) 751.
7. V. Chauvaut, PhD thesis, University of Paris VI (ENSCP), France (1998).
8. Y. Mugikura and J.R. Selman, *J. Electrochem. Soc.* **143** (1996) 2442.
9. JCPDS, file 29-0801.
10. V. Chauvaut and M. Cassir, *J. Electroanal. Chem.* **474** (1999) 9.
11. S. Garnier, C. Bohnke, O. Bohnke and J.L. Fourquet, *Solid State Ionics.* **83** (1996) 323.
12. M. Stromme Mattson, A. Azens, G.A. Niklasson and C.G. Granqvist, *J. Appl. Phys.* **81** (1997) 6432.